© 2018. Published by The Company of Biologists Ltd | Journal of Cell Science (2018) 131, jcs218743. doi:10.1242/jcs.218743

RESEARCH ARTICLE

Nutritional cell cycle reprogramming reveals that inhibition of Cdk1 is required for proper MBF-dependent transcription

Angela Rubio[1,2,*], Natalia García-Blanco[1,2], Alicia Vázquez-Bolado[1,2], María Belén Suárez[1,2] and Sergio Moreno[1,‡]

ABSTRACT

In nature, cells and in particular unicellular microorganisms are exposed to a variety of nutritional environments. Fission yeast cells cultured in nitrogen-rich media grow fast, divide with a large size and show a short G1 and a long G2. However, when cultured in nitrogen-poor media, they exhibit reduced growth rate and cell size and a long G1 and a short G2. In this study, we compared the phenotypes of cells lacking the highly conserved cyclin-dependent kinase (Cdk) inhibitor Rum1 and the anaphase-promoting complex/cyclosome (APC/C) activator Ste9 in nitrogen-rich and nitrogen-poor media. Rum1 and Ste9 are dispensable for cell division in nitrogen-rich medium. However, in nitrogen-poor medium they are essential for generating a proper wave of MluI cell-cycle box binding factor (MBF)-dependent transcription at the end of G1, which is crucial for promoting a successful S phase. Mutants lacking Rum1 and Ste9 showed premature entry into S phase and a reduced wave of MBF-dependent transcription, leading to replication stress, DNA damage and G2 cell cycle arrest. This work demonstrates how reprogramming the cell cycle by changing the nutritional environment may reveal new roles for cell cycle regulators.

KEY WORDS: Cell growth, Cell cycle, Nitrogen, Rum1, Ste9, MBF, *Schizosaccharomyces pombe*

INTRODUCTION

The nutritional environment determines the growth rate, cell size and cell cycle distribution. Because most laboratories use nutrient-rich media to grow cells, most published studies were performed under conditions of maximal growth. Fission yeast cells constantly monitor the nutritional environment, in particular nitrogen content, in order to coordinate cell growth with cell division and cell differentiation. In the presence of nitrogen, fission yeast cells grow and divide; in the complete absence of nitrogen, they stop growing and undergo cell cycle arrest and differentiation (Yanagida, 2009). Most laboratories grow fission yeast cells in nitrogen-rich media, where cells grow fast and divide with a large cell size after a long G2 phase. However, fission yeast cells can also grow and divide in nitrogen-poor media. When fission yeast cells are shifted from nitrogen-rich to nitrogen-poor medium their cell cycle is immediately reprogrammed and they divide with a small cell size. In this nitrogen-poor environment, G2 is short and G1 is long (Fantes and Nurse, 1977; Carlson et al., 1999; Petersen and Nurse, 2007; Chica et al., 2016).

Recently, our group has shown that the Greatwall (Ppk18 and Cek1 in fission yeast)–Endosulfine (Igo1 in fission yeast)–PP2A/B55 (Ppa1/Pab1 and Ppa2/Pab1 in fission yeast) pathway couples cell growth to the mitotic cell cycle machinery by regulating the activity of PP2A/B55, the main protein phosphatase that dephosphorylates the cyclin-dependent kinase-1 (Cdk1)/cyclinB substrates in fission yeast (Chica et al., 2016; Pérez-Hidalgo and Moreno, 2017). In nitrogen-rich media, TORC1 and PP2A/B55 activities are high and G2 is long; as a consequence, the cells are large. In nitrogen-poor media, TORC1 and PP2A/B55 activities are low, the cells enter mitosis with a reduced cell size, G2 is short and G1 is extended to maintain cell size homeostasis.

Extension of G1 in fission yeast depends on the presence of Rum1 and Ste9, two negative cell cycle regulators that maintain a low CDK activity during G1 before entry into S phase. Rum1 is a CDK inhibitor (CKI) of Cdk1/cyclin B complexes (Moreno and Nurse, 1994; Correa-Bordes et al., 1997; Benito et al., 1998), whereas Ste9 (initially named Srw1) is an activator of the anaphase-promoting complex/cyclosome (APC/C) that promotes the degradation of the B-type cyclins in G1 (Yamaguchi et al., 1997, 2000; Kitamura et al., 1998; Kominami et al., 1998; Blanco et al., 2000; Yamano et al., 2000). Cells lacking Rum1 and Ste9 divide with the same size and with the same generation time as wild-type cells (Moreno and Nurse, 1994; Yamaguchi et al., 1997; Kitamura et al., 1998; Kominami et al., 1998), indicating that Rum1 and Ste9 are dispensable in nitrogen-rich media. However, Rum1 and Ste9 are required for G1 arrest and for mating in minimal medium without nitrogen (Moreno and Nurse, 1994; Correa-Bordes et al., 1997; Benito et al., 1998; Kitamura et al., 1998; Blanco et al., 2000; Stern and Nurse, 1998; Martín-Castellanos et al., 2000).

Oscillatory changes in Cdk1 activity are sufficient to entrain periodic transcription through the cell cycle (Banyai et al., 2016). One of these transcription factors, MluI cell-cycle box (MCB) binding factor (MBF), the functional orthologue of mammalian E2F, regulates the expression of genes involved in the G1/S transition, such as *cig2*$^{+}$ encoding the main G1/S cyclin, and in DNA replication, such as *cdc18*$^{+}$, *cdt1*$^{+}$ or *cdc22*$^{+}$ (Baum et al., 1997; Kelly et al., 1993; Fernández-Sarabia et al., 1993; Hofmann and Beach, 1994; Lowndes et al., 1992; Ayté et al., 2001; Maqbool et al., 2003).

Here, we show that Rum1 and Ste9 proteins are essential in cells growing in nitrogen-poor media. In this nutritional environment, cells lacking Rum1 and Ste9 show premature entry into S phase, with reduced MBF activity. Rum1 and Ste9 are required to extend the G1 phase of the cell cycle by inhibiting Cdk1 activity and to set a proper wave of MBF activity at G1/S, which is crucial in providing high levels of expression of S phase genes in order to avoid DNA

[1]Instituto de Biología Funcional y Genómica, CSIC, University of Salamanca, 37007 Salamanca, Spain. [2]Department of Microbiology and Genetics, University of Salamanca, 37007 Salamanca. Spain.
*Present address: Department of Biochemistry, University of Cambridge, Cambridge CB2 1QW, UK.

‡Author for correspondence (smo@usal.es)

S.M., 0000-0002-8039-1413

Received 9 April 2018; Accepted 20 August 2018

Journal of Cell Science (2018) 131, jcs218743. doi:10.1242/jcs.218743

damage during S phase and G2. Therefore, under nitrogen restriction, inhibition of Cdk1 in G1 is essential in order to entrain MBF-dependent transcription at the onset of S phase.

RESULTS

Fission yeast Rum1 and Ste9 are essential for extending G1 in nitrogen-poor medium

Fission yeast has two cell size controls, one operating at the end of G1 before the onset of S phase and the other at the end of G2, before mitosis. In nitrogen-rich medium, EMM2 (Edinburgh minimal medium with 5 g l^{-1} NH_4Cl) or MMGlu (Edinburgh minimal medium with 20 mM glutamate), the cell size required to initiate mitosis is about 14 µm. In this nutritional environment, the G2/M size control predominates and the G1/S cell size control is cryptic because the newly born daughter cells are larger than the minimal cell size required to initiate S phase. In nitrogen-poor medium, MMPhe (Edinburgh minimal medium with 20 mM phenylalanine as nitrogen source), wild-type fission yeast cells initiate mitosis with approximately 10 µm cell size, generating two daughter cells with a smaller cell size than the minimum required to initiate S phase. In this poor nutritional environment, fission yeast cells extend the G1 phase and grow until they reach the minimum cell size required to initiate S phase (Fig. S1, wt) (Nurse, 1975; Nurse et al., 1976; Nurse and Thuriaux, 1977; Nasmyth et al., 1979; Sveiczer et al., 1996).

In order to understand the molecular basis and the relevance of this G1 extension, we shifted wild-type fission yeast cells from a nitrogen-rich medium (MMGlu) to a nitrogen-poor medium (MMPhe) and determined the protein levels of Rum1 and Ste9, two functionally conserved G1 cell cycle inhibitors. Four hours after the shift, Rum1 protein levels increased in MMPhe, albeit not as much as in minimal medium without nitrogen (MM-N) (Fig. 1A, left panel) (Martín-Castellanos et al., 2000; Daga et al., 2003). In the same experiment, the Ste9 protein showed a shift in mobility (Fig. 1A, right panel), suggesting that it became dephosphorylated in MMPhe, as previously described in MM-N (Fig. 1A, right panel) (Blanco et al., 2000). Consistent with the accumulation of Rum1 and the dephosphorylation of Ste9, a 1C G1 population was observed 4 h after the shift, both in MMPhe and in MM-N (Fig. 1B and Fig. S1).

Unlike wild-type cells, mutant cells lacking *rum1*$^+$, *ste9*$^+$ or both *rum1*$^+$ and *ste9*$^+$ did not show the 1C G1 population in MMPhe. Instead, these mutants showed a population of cells with a DNA content between 1C and 2C, most likely corresponding to cells in S phase (Fig. 1C and Fig. S1, arrowheads). The double mutant *rum1Δ ste9Δ* showed more cells in S phase than the single mutants *rum1Δ* or *ste9Δ*.

To confirm that there were more cells in S phase in cells lacking Rum1 and Ste9 than in the wild type, we shifted wild-type and *rum1Δ ste9Δ* mutant cells from MMGlu to MMPhe and determined the percentage of cells in S phase by measuring the incorporation of the thymidine analogue 5-bromo-2′-deoxyuridine (BrdU) in fission yeast cells expressing the thymidine kinase gene. This nutritional downshift partially synchronises fission yeast cells because 30–40% of the cells are advanced into mitosis as a consequence of the inhibition of PP2A/B55, after the activation of Greatwall–Endosulfine pathway (Chica et al., 2016). The *rum1Δ ste9Δ* mutant showed more BrdU-positive cells than the wild type at different times after the nutritional shift, in particular during the first cell cycle in MMPhe (2 and 4 h) (Fig. 1D). This result revealed that the *rum1Δ ste9Δ* mutant is unable to delay the G1 phase of the cell cycle in MMPhe and shows premature entry into S phase. Taken together, the data indicate that Rum1 and Ste9 are required to extend the G1 phase of the cell cycle and to prevent premature S phase entry in nitrogen-poor medium.

Cells lacking Rum1 and/or Ste9 undergo DNA replication stress in nitrogen-poor medium

Cells deleted for *rum1*$^+$ and/or *ste9*$^+$ behave similarly to wild-type cells and do not show any apparent phenotypes in nitrogen-rich media (Moreno and Nurse, 1994; Yamaguchi et al., 1997; Kitamura et al., 1998; Kominami et al., 1998; Blanco et al., 2000). When *rum1Δ ste9Δ* cells were shifted from MMGlu to MMPhe, they initially underwent cell size reduction similar to that seen for wild-type cells (Fig. 2A,B; 6 h, corresponding to the first cell cycle in MMPhe) but eventually they became elongated (Fig. 2A,B; 13 and 20 h, corresponding to the second and third cell cycles in MMPhe). The number of elongated cells in the *rum1Δ ste9Δ* culture increased steadily over time in MMPhe.

In fission yeast, cells accumulating unrepaired DNA lesions activate the DNA damage checkpoint to delay the cell cycle in G2 in order to repair the damaged DNA before mitosis (Caspari and Carr, 1999). Flow cytometry analysis confirmed that the elongated cells in *rum1Δ ste9Δ* were delayed in G2 (Fig. S2A, lower panel; Fig. S2B). Moreover, the *rum1Δ ste9Δ* mutant showed a high number of small cells with a DNA content between 1C and 2C (Figs S1 and S2C). This new population of cells seems to be the consequence of a slow S phase. To investigate the generation of DNA damage, we monitored the formation of Rad52:YFP nuclear foci that accumulate at the sites of double-strand breaks or collapsed DNA replication forks (Kim et al., 2000; Meister et al., 2005). The *rum1Δ ste9Δ* mutant cells began to accumulate Rad52:YFP nuclear foci after the first cell cycle in MMPhe (Fig. 2C,D; 6 h); the number and intensity of the foci and the percentage of elongated cells increased over time. After 24–48 h in MMPhe, about 50% of the cells were elongated and contained very intense Rad52:YFP foci (Fig. 2C,D). Cell elongation and Rad52:YFP nuclear foci were also observed in *rum1Δ* and *ste9Δ* single mutants after 20–48 h in MMPhe (Fig. S3A,B). Cells lacking Rum1 showed a percentage of Rad52:YFP foci very close to that of the double mutant *rum1Δ ste9Δ*, whereas in cells lacking Ste9 the percentage of Rad52:YFP foci was intermediate, between the wild type and *rum1Δ* (Fig. S3C). This result indicates that Rum1 plays a major role and Ste9 a minor role in preventing DNA damage in nitrogen-poor medium.

Elongated *rum1Δ ste9Δ* cells in MMPhe activate the DNA damage checkpoint

The fission yeast serine-threonine protein kinase ATR homologue, Rad3, is activated in response to DNA damage (Brondello et al., 1999). We examined the phenotype of the *rad3Δ rum1Δ ste9Δ* triple mutant in MMPhe. These cells showed a significant reduction in the number of elongated cells after 20 h in MMPhe compared with the double mutant *rum1Δ ste9Δ* (Fig. 3A,B), suggesting that the cell cycle delay in G2 was dependent on Rad3. As shown in Fig. 3C, *rad3Δ rum1Δ ste9Δ* mutant cells presented a significant percentage of cut and mis-segregation phenotypes, reminiscent of cells undergoing mitotic catastrophe. Moreover, flow cytometry analysis revealed a sub-G1 population of dead cells in the triple mutant *rad3Δ rum1Δ ste9Δ* that was not observed in the double mutant *rum1Δ ste9Δ* (Fig. 3D, arrow). Deletion of *rad3*$^+$ also decreased the fitness of *rum1Δ ste9Δ* cells in MMPhe (Fig. S4). Together, these results suggest that the Rad3 protein kinase is required for the cell cycle delay in G2 necessary to allow the survival of cells lacking Rum1 and Ste9 in MMPhe.

Journal of Cell Science (2018) 131, jcs218743. doi:10.1242/jcs.218743

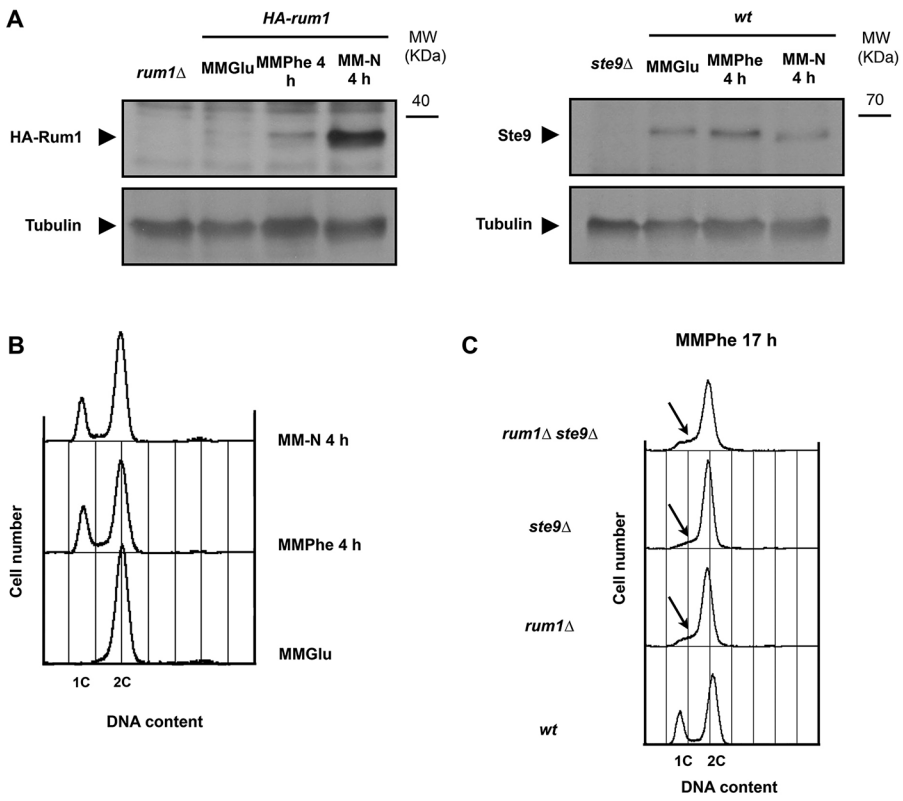

Fig. 1. Rum1 and Ste9 are essential for G1 extension in nitrogen-poor medium. Wild-type (wt), *HA-rum1*, *rum1Δ*, *ste9Δ* and *rum1Δ ste9Δ* cells were shifted from MMGlu to MMPhe or to MM-N. (A) Western blot using anti-Rum1 (left panel) or anti-Ste9 (right panel) antibodies. Tubulin was used as a protein loading control. (B) FACS profile showing the DNA content (1C and 2C) of wild-type cells in MMGlu and 4 h after the shift to MMPhe or to MM-N. (C) FACS profile showing the DNA content (1C and 2C) of wild-type, *rum1Δ*, *ste9Δ* and *rum1Δ ste9Δ* cells 17 h after the shift to MMPhe. The arrows mark a population of cells in S phase. (D) Percentage of cells positive for BrdU nuclear staining at different times (0, 2, 4, 6, 8 and 17 h) after the shift from MMGlu to MMPhe. A total of 900 cells were counted at each time point. Wild-type (black), *rum1Δ ste9Δ* (grey).

Rad3 is the apical protein kinase that activates the checkpoint kinases Cds1 and Chk1 in response to DNA replication stress (Cds1) or to DNA breaks (Chk1) (Rhind and Russell, 1998). We compared the phenotypes of the *rum1Δ ste9Δ* cells lacking *rad3*$^{+}$, *chk1*$^{+}$ or *cds1*$^{+}$ after 20 h in MMPhe (Fig. 3E). Cells from the triple mutant *chk1Δ rum1Δ ste9Δ* behaved similarly to *rad3Δ rum1Δ ste9Δ* cells in that they did not elongate and showed a similar percentage of cut and mis-segregation phenotypes (Fig. 3C,F). In fission yeast, activation of Rad3 in response to DNA damage leads to the phosphorylation and activation of Chk1 (Walworth and Bernards, 1996; Wan and Walworth, 2001; Capasso et al., 2002). We observed a mobility shift of phosphorylated Chk1 in two independent clones of *rum1Δ ste9Δ* cells growing in MMPhe for 17 h (Fig. 3G). Mild phosphorylation of Chk1 was detected as early as 4–6 h after the shift from MMGlu to MMPhe (Fig. 3H), indicating that *rum1Δ ste9Δ* cells activate the DNA damage response during the first cell cycle after the shift and that phosphorylation of Chk1 accumulates gradually in nitrogen-poor medium, reaching a maximum after 12 h.

Cds1 is the fission yeast kinase that becomes activated after DNA replication stress and is required to slow down S phase. Cds1 is phosphorylated and activated during S phase by Rad3 in response to DNA replication fork arrest (Lindsay et al., 1998). We failed to detect a band shift of phosphorylated Cds1 protein in *rum1Δ ste9Δ* cells, probably because activation of the DNA replication checkpoint was either weak or transient. Instead, we determined the number of elongated cells and the percentage of cells with Rad52:YFP nuclear foci in the *cds1Δ rum1Δ ste9Δ* triple mutant compared with the *rum1Δ ste9Δ* double mutant after 20 h in MMPhe. As shown in Fig. 3E and Fig. S5A,B, the triple mutant

Journal of Cell Science (2018) 131, jcs218743. doi:10.1242/jcs.218743

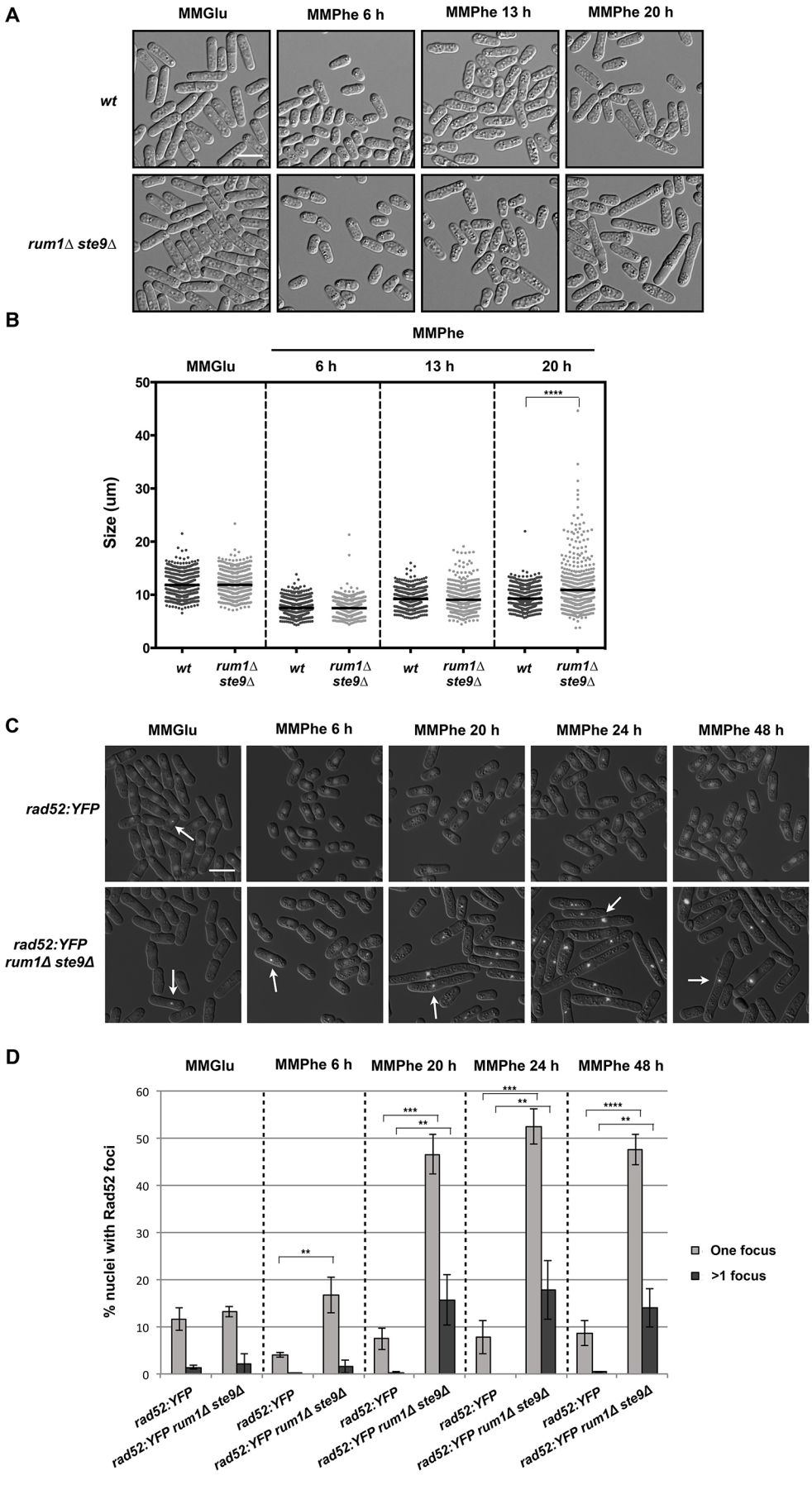

Fig. 2. Cells lacking Rum1 and Ste9 become elongated and accumulate DNA damage in nitrogen-poor medium. Wild-type (wt) and *rum1Δ ste9Δ* mutant cells were shifted from MMGlu to MMPhe. Samples were taken 6, 13 and 20 h after the shift to MMPhe. (A) Differential interference contrast (DIC) microscopy images of live cells. (B) Cell lengths of 600 cells stained with blankophor. The bar represents the average value±s.d. Wild-type (*rad52:YFP*) and *rad52:YFP rum1Δ ste9Δ* cells were shifted from MMGlu to MMPhe. Samples were taken at different times after the shift. (C) Fluorescence microscopy images of Rad52:YFP combined with DIC microscopy in MMGlu at 0, 6, 20, 24 and 48 h after the shift to MMPhe. The arrows indicate cells with Rad52:YFP nuclear foci. (D) Percentage of cells with one (light grey) or more than one nuclear foci (dark grey) of Rad52:YFP at different times (0, 6, 20, 24 and 48 h) after the shift from MMGlu to MMPhe. Three experimental replicas were counted at each time point (n=500 cells per replica and time point). Scale bars: 10 µm. $^{**}P<0.001$, $^{***}P<0.0001$ and $^{****}P<0.00001$.

Journal of Cell Science (2018) 131, jcs218743. doi:10.1242/jcs.218743

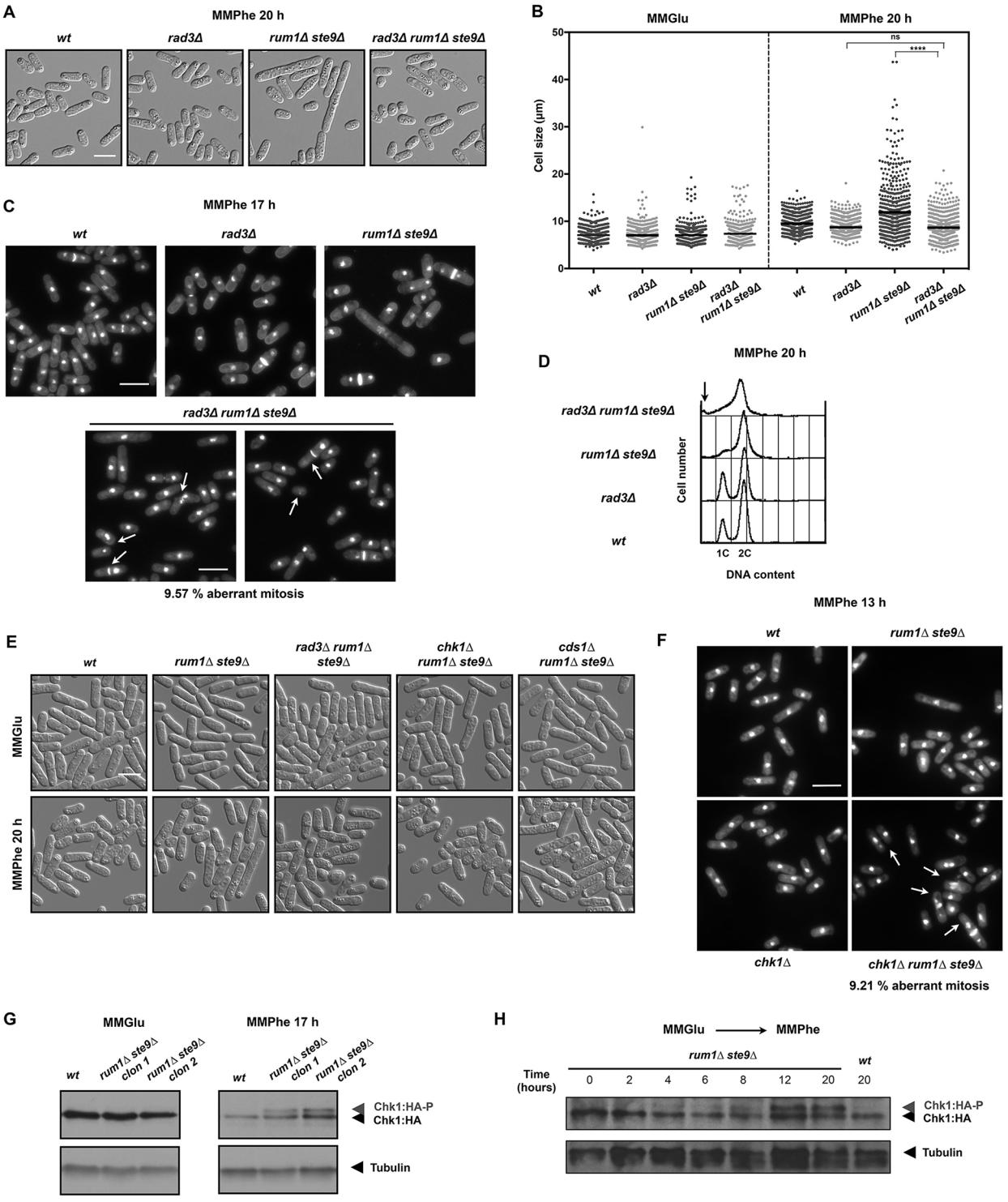

Fig. 3. Cells lacking Rum1 and Ste9 activate the DNA damage checkpoint in nitrogen-poor medium. Wild-type (wt) or mutant cells were grown in MMGlu and then shifted to MMPhe. Samples were taken in MMGlu or at different times after the shift to MMPhe. (A) DIC microscopy images of live wt, *rad3Δ*, *rum1Δ ste9Δ* and *rad3Δ rum1Δ ste9Δ* cells after 20 h in MMPhe. (B) Cell lengths of 600 cells stained with blankophor in MMGlu and 20 h after the shift to MMPhe. The bar represents the average value. (C) Fluorescence microscopy images of cells stained with DAPI and blankophor. Arrows indicate cells showing cut and mis-segregation phenotypes in the *rad3Δ rum1Δ ste9Δ* mutant. (D) FACS profile showing the DNA content (1C and 2C) of wt, *rad3Δ*, *rum1Δ ste9Δ* and *rad3Δ rum1Δ ste9Δ* cells at 20 h after the shift to MMPhe. (E) DIC microscopy images of live wt, *rum1Δ ste9Δ*, *rad3Δ rum1Δ ste9Δ*, *chk1Δ rum1Δ ste9Δ* and *cds1Δ rum1Δ ste9Δ* cells in MMGlu and after 20 h in MMPhe. (F) Fluorescence microscopy images of cells stained with DAPI and blankophor. The arrows indicate cells showing cut and mis-segregation phenotypes in the *chk1Δ rum1Δ ste9Δ* mutant. (G) Western blot using anti-HA antibodies to detect unphosphorylated (fast migrating) and phosphorylated (slow migrating) levels of Chk1 protein in cells growing in MMGlu (left panel) and in MMPhe for 17 h (right panel). Tubulin was used as a protein loading control. (H) Western blot of *chk1:HA rum1Δ ste9Δ* extracts using anti-HA antibodies to detect the levels of unphosphorylated (fast migrating) and phosphorylated (slow migrating) Chk1 protein after a shift from MMGlu to MMPhe. Tubulin was used as a protein loading control. Scale bars: 10 μm. ****P<0.00001, ns, not significant.

Journal of Cell Science (2018) 131, jcs218743. doi:10.1242/jcs.218743

cds1Δ rum1Δ ste9Δ contained more elongated cells and a higher percentage of cells with Rad52:YFP nuclear foci than the double mutant *rum1Δ ste9Δ*. Consistent with this data, the *rum1Δ ste9Δ* mutant showed mild hydroxyurea sensitivity even in nitrogen-rich medium (Fig. S6). Together, these results suggest that in cells lacking Rum1 and Ste9 the Cds1 kinase plays a role in preventing DNA damage during S phase. Therefore, in the absence of Rum1 and Ste9, cells undergo DNA replication stress and activate the two checkpoint kinases, Cds1 and Chk1, leading to a slow S phase caused by mild activation of Cds1 and to a cell cycle delay in G2 as a result of activation of Chk1.

Reduced CDK1 or increased PP2A phosphatase activities decrease the DNA damage phenotype of *rum1Δ ste9Δ* cells

Rum1 and Ste9 are negative regulators of Cdk1 activity in G1. Therefore, *rum1Δ ste9Δ* cells should have higher Cdk1 activity than wild-type cells. To test whether Cdk1 upregulation in *rum1Δ ste9Δ* cells is the main cause of genomic instability in MMPhe, we analysed the phenotype of cells with reduced Cdk1 activity. For this purpose we used the analogue-sensitive (as) *cdc2-asM17* allele that encodes a protein that can be inhibited by bulky ATP analogues (Aoi et al., 2014). We observed that *cdc2-asM17* is a hypomorphic allele of *cdc2* because cells expressing this mutant version of *cdc2*$^{+}$ were slightly larger than wild-type cells in MMGlu and in MMPhe, even in the absence of ATP analogue inhibitors (Fig. 4A,B). The reduced Cdk1 activity of this mutant should affect primarily the G2/M transition, which has a threshold of Cdk1 activity higher than the G1/S transition (Coudreuse and Nurse, 2010). Thus, we reasoned that the *cdc2-asM17* cells are larger because they have an extended G2 phase.

As shown in Fig. 4A–C, the *cdc2-asM17 rum1Δ ste9Δ* mutant showed fewer elongated cells and less DNA damage (measured as percentage of cells with Rad52:YFP nuclear foci) after 20 h in MMPhe than *rum1Δ ste9Δ* mutant cells. Consistent with this observation, flow cytometry analysis showed that the *cdc2-asM17 rum1Δ ste9Δ* cells did not contain the population of cells in S phase characteristic of the *rum1Δ ste9Δ* mutant (Fig. 4D). These results indicate that extension of G2 by reducing Cdk1 activity in cells lacking Rum1 and Ste9 may favour DNA repair before mitosis. A long G2 could be one of the reasons why *rum1Δ ste9Δ* cells do not show any apparent phenotypes in nitrogen-rich medium.

At the onset of mitosis, Cdk1/cyclinB kinase activity is opposed by PP2A/B55 phosphatase activity that inhibits Cdk1/cyclinB activation and antagonizes the phosphorylation of downstream targets of Cdk1 (Chica et al., 2016; Pérez-Hidalgo and Moreno, 2017). Deletion of the *ppa2*$^{+}$ gene, encoding one of the two catalytic subunits of PP2A, generates cells smaller than wild-type cells (Fig. 5A,B). This semi-*wee* phenotype is caused by an accelerated entry into mitosis (Chica et al., 2016; Kinoshita et al., 1993; Navarro and Nurse, 2012). Thus, *ppa2Δ* cells showed greater 1C G1 population in MMPhe as an indirect effect of shortening G2 (Fig. 5C). We therefore tested the effect of deleting *ppa2*$^{+}$ in *rum1Δ ste9Δ*. In MMPhe, we observed an increase in the number of elongated cells in *ppa2Δ rum1Δ ste9Δ* mutant cells compared with *rum1Δ ste9Δ*. The difference in cell size between *ppa2Δ rum1Δ ste9Δ* and *ppa2Δ* was larger than between *rum1Δ ste9Δ* and the wild type (2.31 versus 1.85 µm), although the *ppa2Δ rum1Δ ste9Δ* mutant cells did not reach sizes as large as those of the *rum1Δ ste9Δ* mutant (Fig. 5A,B). In addition, there was an increase in the number of cells undergoing DNA replication in the triple mutant *ppa2Δ rum1Δ ste9Δ* compared with the double mutant *rum1Δ ste9Δ* (Fig. 5C, arrows). Importantly, 7.29% of the *ppa2Δ rum1Δ ste9Δ*

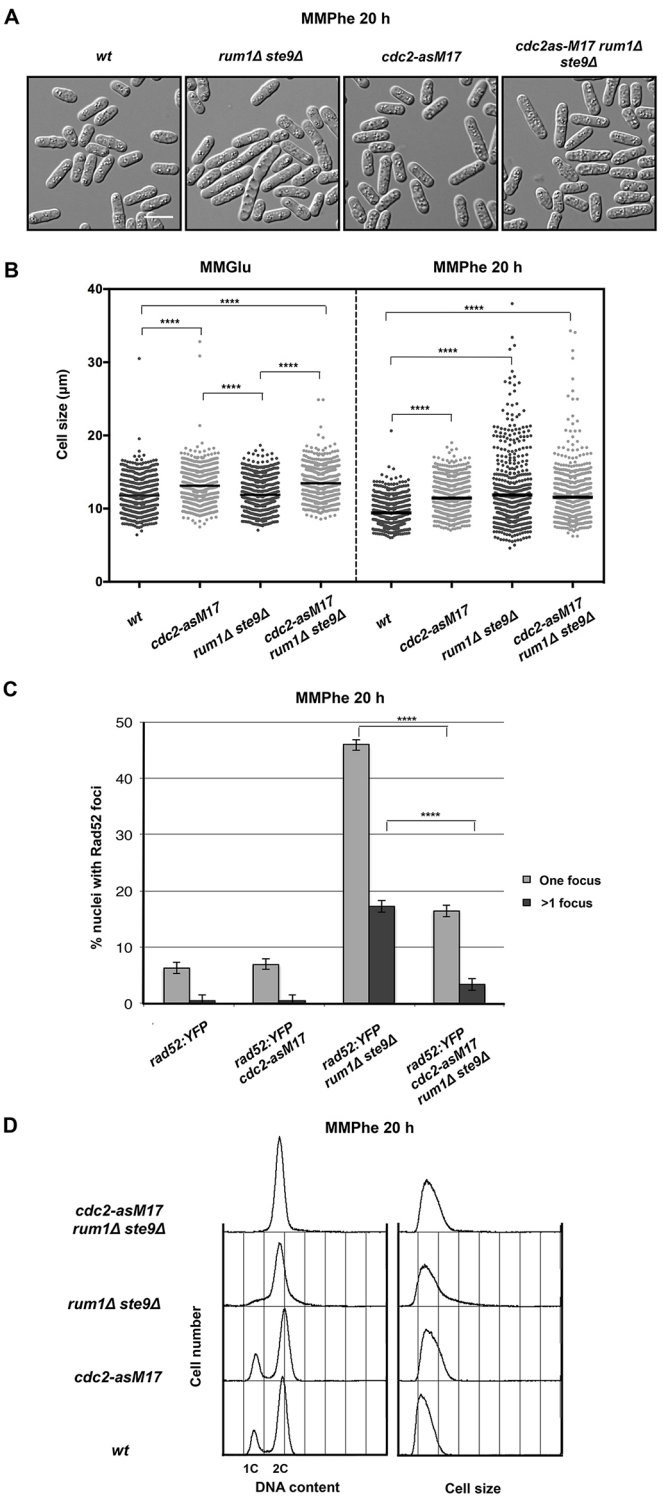

Fig. 4. Reduced Cdk1 activity rescues the *rum1Δ ste9Δ* DNA damage phenotype in nitrogen-poor medium. Wild-type (wt), *cdc2-asM17*, *rum1Δ ste9Δ* and *cdc2-asM17 rum1Δ ste9Δ* mutant cells were grown in MMGlu and then shifted to MMPhe for 20 h. (A) DIC microscopy images of live cells after 20 h in MMPhe. Scale bar: 10 µM. (B) Cell lengths of 600 cells stained with blankophor growing in MMGlu or in MMPhe for 20 h. The bar represents the average value. (C) Percentage±s.d. of cells with one (light grey) or more than one Rad52:YFP nuclear foci (dark grey) after 20 h of growth in MMPhe. Three experimental replicas were counted at each time point (n=500 cells per replica and time point). (D) FACS profile showing the DNA content (1C and 2C) and the cell size (forward scatter) of wt, *cdc2-asM17*, *rum1Δ ste9Δ* and *cdc2-asM17 rum1Δ ste9Δ* cells 20 h after the shift to MMPhe. ****P<0.00001.

Journal of Cell Science (2018) 131, jcs218743. doi:10.1242/jcs.218743

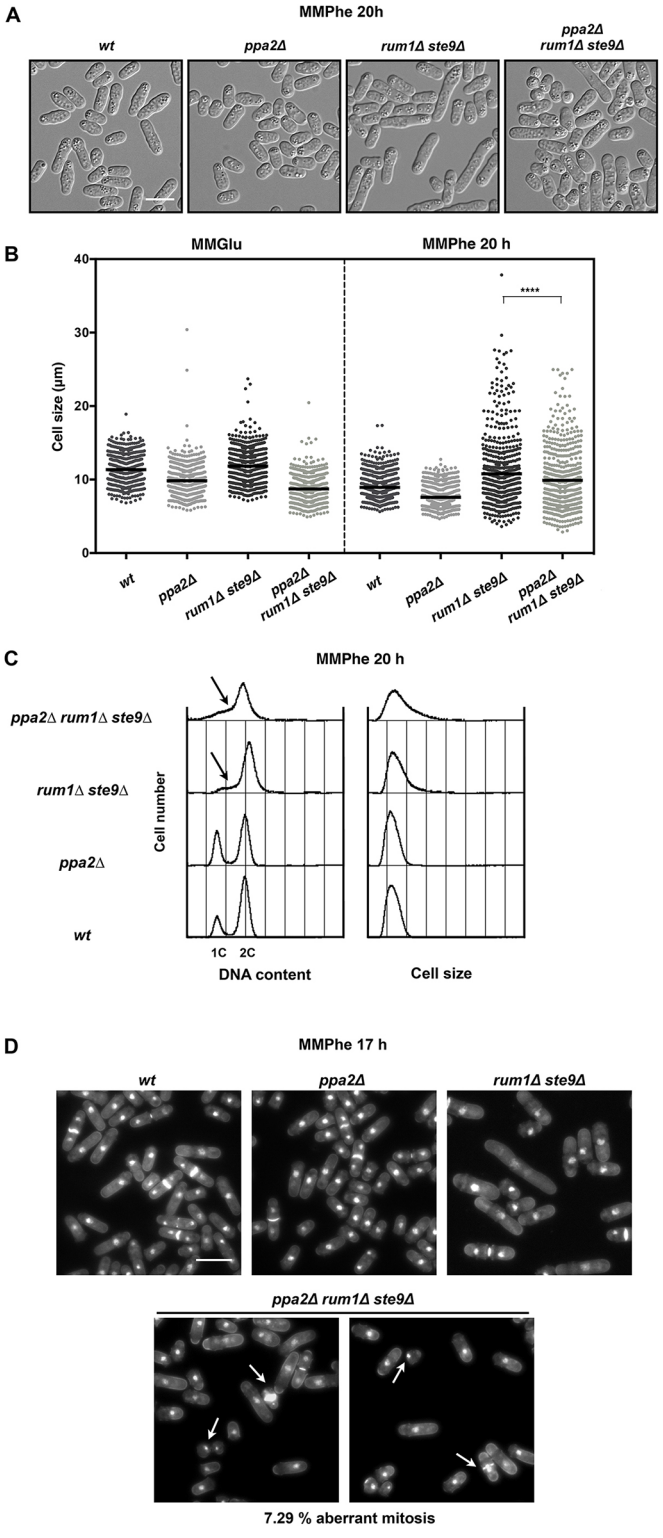

Fig. 5. Reduced PP2A activity aggravates the *rum1Δ ste9Δ* DNA damage phenotype in nitrogen-poor medium. Wild-type (wt), *ppa2Δ*, *rum1Δ ste9Δ* and *ppa2Δ rum1Δ ste9Δ* mutant cells were grown in MMGlu and then shifted to MMPhe for 20 h. (A) DIC microscopy images of live cells after 20 h in MMPhe. (B) Cell lengths of 600 cells stained with blankophor growing in MMGlu or in MMPhe for 20 h. The bar represents the average value. (C) FACS profile showing the DNA content (1C and 2C) and the cell size (forward scatter) of wt, *ppa2Δ*, *rum1Δ ste9Δ* and *ppa2Δ rum1Δ ste9Δ* cells 20 h after the shift to MMPhe. The arrows mark a population of cells in S phase. (D) Fluorescence microscopy images of cells stained with DAPI and blankophor. Arrows indicate cells showing cut and mis-segregation phenotypes in the *ppa2Δ rum1Δ ste9Δ* mutant. Scale bars: 10 µm. ****P<0.00001.

mutant cells showed cut and mis-segregation phenotypes in MMPhe (Fig. 5D), a slightly smaller percentage than *rad3Δ rum1Δ ste9Δ* (9.57%) (Fig. 3C) or *chk1Δ rum1Δ ste9Δ* cells (9.21%) (Fig. 3F). These results indicate that a reduction in PP2A activity in the *rum1Δ ste9Δ* mutant increases the number of cells delayed by the checkpoint and that some of these cells are unable to maintain the cell cycle arrest. These cells enter into mitosis and undergo mitotic catastrophe, indicating that PP2A activity is also important in preventing entry into mitosis in response to the activation of the DNA damage checkpoint, suggesting that both inhibition of Cdk1/cyclin B and activation of PP2A are required to delay the cell cycle in G2 upon DNA damage. In agreement with this idea, upregulation of PP2A phosphatase activity in the presence of DNA damage has been described in *Xenopus* egg extracts (Wang et al., 2015).

Deletion of *spd1*$^+$ partially rescues the DNA damage phenotype of *rum1Δ ste9Δ* cells

The correct supply of deoxyribonucleoside triphosphates (dNTPs) during S phase is crucial in maintaining genome integrity (Chabes and Stillman, 2007; Fleck et al., 2013). Recently, it has been shown that reduced MBF-dependent ribonucleotide reductase (RNR) expression generates DNA replication stress and checkpoint activation, phenotypes that can be reversed by increasing the dNTP pools (Pai et al., 2017). Low levels of RNR provide sufficient dNTPs for mitochondrial DNA synthesis and for DNA repair in quiescent cells and during the G1 phase of the cell cycle, but RNR levels and activity have to increase to high levels as cells enter S phase (Stillman, 2013).

In fission yeast, Spd1 inhibits assembly of RNR in G1. Spd1 is later degraded when the cells enter S phase or in response to DNA replication stress, which activates RNR to increase the dNTP pools (Liu et al., 2003, 2005; Håkansson et al., 2006). Therefore, we tested whether deletion of *spd1*$^+$ could rescue the DNA damage phenotype of the *rum1Δ ste9Δ* cells in MMPhe by increasing the dNTP pools. We observed that *rum1Δ ste9Δ spd1Δ* cells were less elongated (Fig. 6A), showed less DNA damage (Fig. 6B) and grew slightly better in MMPhe (Fig. S4) than *rum1Δ ste9Δ*. This result suggests that *rum1Δ ste9Δ* cells may have a problem at the onset of S phase that leads to a reduction in the dNTP pools.

MBF-dependent transcription is deregulated in *rum1Δ ste9Δ* cells

It has been shown that increasing the dNTP pools rescues the DNA damage phenotype of the *rum1Δ ste9Δ* double mutant; expression of *cdc22*$^+$, encoding the large subunit of RNR, at G1/S is MBF-dependent; Spd1 is targeted for degradation by the CRL4-Cdt2 ubiquitin ligase at the onset of S phase; and Cdt2 is also a target of the MBF transcription factor (Hofmann and Beach, 1994; Liu et al., 2003, 2005; Håkansson et al., 2006; Holmberg et al., 2005). We therefore reasoned that defective MBF activation could be responsible for the reduced expression of RNR and for high levels of Spd1. Taking all this into account, we decided to explore the activity of the MBF transcription factor in wild-type and *rum1Δ ste9Δ* mutant cells growing in nitrogen-poor medium. MBF, the fission yeast functional orthologue of mammalian E2F, promotes transcription of cell cycle genes at the end of G1. Most MBF target genes encode proteins involved in the initiation of DNA replication, nucleotide biogenesis and the regulation of S phase (Bähler, 2005). Deregulation of MBF promotes genotoxic stress in S phase (Pai et al., 2017; Caetano et al., 2014; Pfister et al., 2015).

To test whether MBF-dependent transcription was affected in the *rum1Δ ste9Δ* mutant, we monitored the levels of two MBF targets

Journal of Cell Science (2018) 131, jcs218743. doi:10.1242/jcs.218743

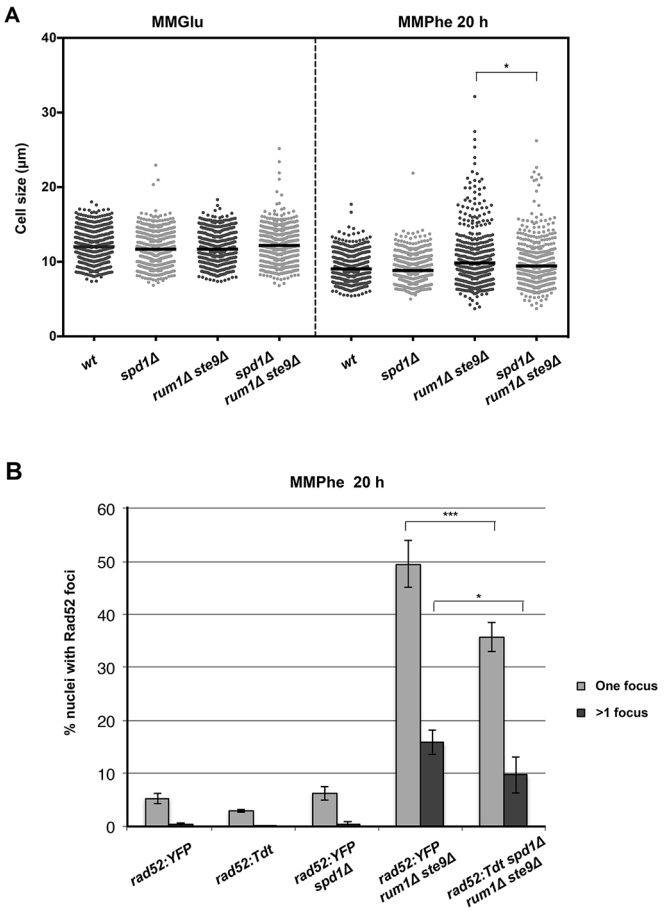

Fig. 6. Deletion of *spd1*$^{+}$ partially rescues the *rum1Δ ste9Δ* DNA damage phenotype in nitrogen-poor medium. Wild-type (wt), *spd1Δ*, *rum1Δ ste9Δ* and *spd1Δ rum1Δ ste9Δ* mutant cells were grown in MMGlu and then shifted to MMPhe for 20 h. (A) Cell lengths of 600 cells stained with blankophor growing in MMGlu or in MMPhe for 20 h. (B) Percentage±s.d. of cells with one (light grey) or more than one nuclear foci (dark grey) of Rad52:YFP, after 20 h of growth in MMPhe. Three experimental replicas were counted at each time point (*n*=500 cells per replica and time point). **P*<0.01, ****P*<0.0001, *****P*<0.00001.

(*cdc18*$^{+}$ and *cdc22*$^{+}$ mRNAs) using real-time quantitative polymerase chain reaction (RT-qPCR) in wild-type and *rum1Δ ste9Δ* cells at different times after the shift from MMGlu to MMPhe. As shown in Fig. 7A (left panel), *cdc18*$^{+}$ and *cdc22*$^{+}$ mRNA levels rose to a peak 4 h after the shift from nitrogen-rich (MMGlu) to nitrogen-poor (MMPhe) medium, when cells are undergoing S phase (Fig. 1B,C). Both *cdc18*$^{+}$ and *cdc22*$^{+}$ mRNA levels were significantly reduced in the *rum1Δ ste9Δ* mutant cells compared with the wild type (Fig. 7A). In nitrogen-rich medium (MMGlu, time 0), the levels of *cdc18*$^{+}$ and *cdc22*$^{+}$ mRNAs were slightly but reproducibly reduced in *rum1Δ ste9Δ* mutant cells compared with the wild type. After 4 h in nitrogen-poor medium, the mRNA levels of *cdc18*$^{+}$ and *cdc22*$^{+}$ dropped considerably in *rum1Δ ste9Δ* mutant cells (Fig. 7A). As a control, we determined the mRNA levels of *cdc18*$^{+}$ and *cdc22*$^{+}$ in cells lacking Rep2 (*rep2Δ*), a positive regulator of MBF that shows reduced MBF-dependent transcription (Fig. 7A, right panel) (Baum et al., 1997; Gaspa et al., 2016; Tournier and Millar, 2000).

We also monitored the levels of the Tos4 protein, another MBF target (Kiang et al., 2009), by western blot in wild-type and *rum1Δ ste9Δ* mutant cells in a similar time course experiment to that described above. In nitrogen-poor medium (MMPhe), Tos4:GFP protein levels were significantly reduced in the *rum1Δ ste9Δ* mutant compared with levels in wild-type cells (Fig. 7B). Again, in nitrogen-rich medium (MMGlu, time 0), *rum1Δ ste9Δ* mutant cells contained reduced levels of Tos4:GFP protein compared with wild-type cells (Fig. 7B). Moreover, we counted the number of Tos4:GFP-positive cells using fluorescent microscopy in MMGlu and at 3 and 4 h after the shift to MMPhe. As shown in Fig. 7C, in MMGlu and 3 or 4 h after the shift to MMPhe, *rum1Δ ste9Δ* cells showed fewer Tos4:GFP-positive cells than the wild type. In addition, the Tos4:GFP signal was less intense in the *rum1Δ ste9Δ* mutant than in the wild-type strain (Fig. 7D). Together, these results are consistent with a reduction in the amplitude of the MBF-dependent expression wave in cells lacking Rum1 and Ste9 in comparison with wild-type cells.

Reduced MBF-dependent transcription leads to DNA damage in poor medium

The core MBF transcription factor is composed of Cdc10 and the DNA-binding proteins Res1 and Res2. Additionally, Rep2 is a co-activator of MBF that it is required for high levels of MBF-dependent transcription, but not for transcription periodicity (Baum et al., 1997; Whitehall et al., 1999; Ayté et al., 1995; Zhu et al., 1997; Tahara et al., 1998). Nrm1 and Yox1 are co-repressors of MBF, forming part of a negative feedback loop to repress MBF activity in S phase, G2 and mitosis. Nrm1 and Yox1 accumulate during S phase, bind to MBF at promoters and repress MBF-dependent transcription outside of G1 (de Bruin et al., 2008; Caetano et al., 2011; Ivanova et al., 2011; Aligianni et al., 2009; Purtill et al., 2011). Deletion of *nrm1*$^{+}$ increases MBF-dependent transcription, resulting in replication errors and genomic instability (Caetano et al., 2014).

We compared the phenotypes of wild-type, *rum1Δ ste9Δ, rep2Δ* (with downregulated MBF activity) and *nrm1Δ* (with upregulated MBF activity) cells in MMGlu and after 20 h in MMPhe. In nitrogen-rich medium (MMGlu), *nrm1Δ* mutant cells were larger than wild-type cells (Fig. 8A,B), showed a high percentage of nuclei with Rad52:YFP nuclear foci in MMGlu (Fig. 8C) and exhibited activation of Chk1, as previously described by Caetano et al. (2014). Interestingly, in nitrogen-poor medium (MMPhe), the phenotype of the *nrm1Δ* mutant was similar to the wild type (Fig. 8A,B), whereas cells lacking Rep2 presented a marked increase in cell size and high percentage of Rad52:YFP nuclear foci (Fig. 8A–C), similar to the *rum1Δ ste9Δ* mutant. Flow cytometry analysis revealed that the *nrm1Δ* mutant did not display a G1 population in MMPhe (Fig. 8D) because they divided with a greater cell size than wild-type cells (Fig. 8A,B). By contrast, the *rep2Δ* mutant presented more cells with 1C DNA content peak than the wild type as a result of delay in S phase entry (Fig. 8D).

Therefore, cells lacking Rep2 showed similar levels of DNA damage in MMPhe to the *rum1Δ ste9Δ* mutant (Fig. 8C). These results indicate that proper MBF regulation is important for maintaining genome integrity, and that downregulation of MBF in nitrogen-poor media has worse consequences than upregulation of MBF.

Deletion of *nrm1* rescues the genomic instability of *rum1Δ ste9Δ* mutant cells

It has been reported that *nrm1Δ* cells exhibit upregulated MBF activity (Gaspa et al., 2016; Caetano et al., 2014). We constructed the triple mutant *nrm1Δ rum1Δ ste9Δ* to test whether upregulation of MBF by deleting *nrm1*$^{+}$ could rescue the DNA damage phenotype of *rum1Δ ste9Δ* mutant cells. As shown in Fig. S7A, the *nrm1Δ rum1Δ ste9Δ* cells were shorter than *rum1Δ ste9Δ* cells in MMPhe

Journal of Cell Science (2018) 131, jcs218743. doi:10.1242/jcs.218743

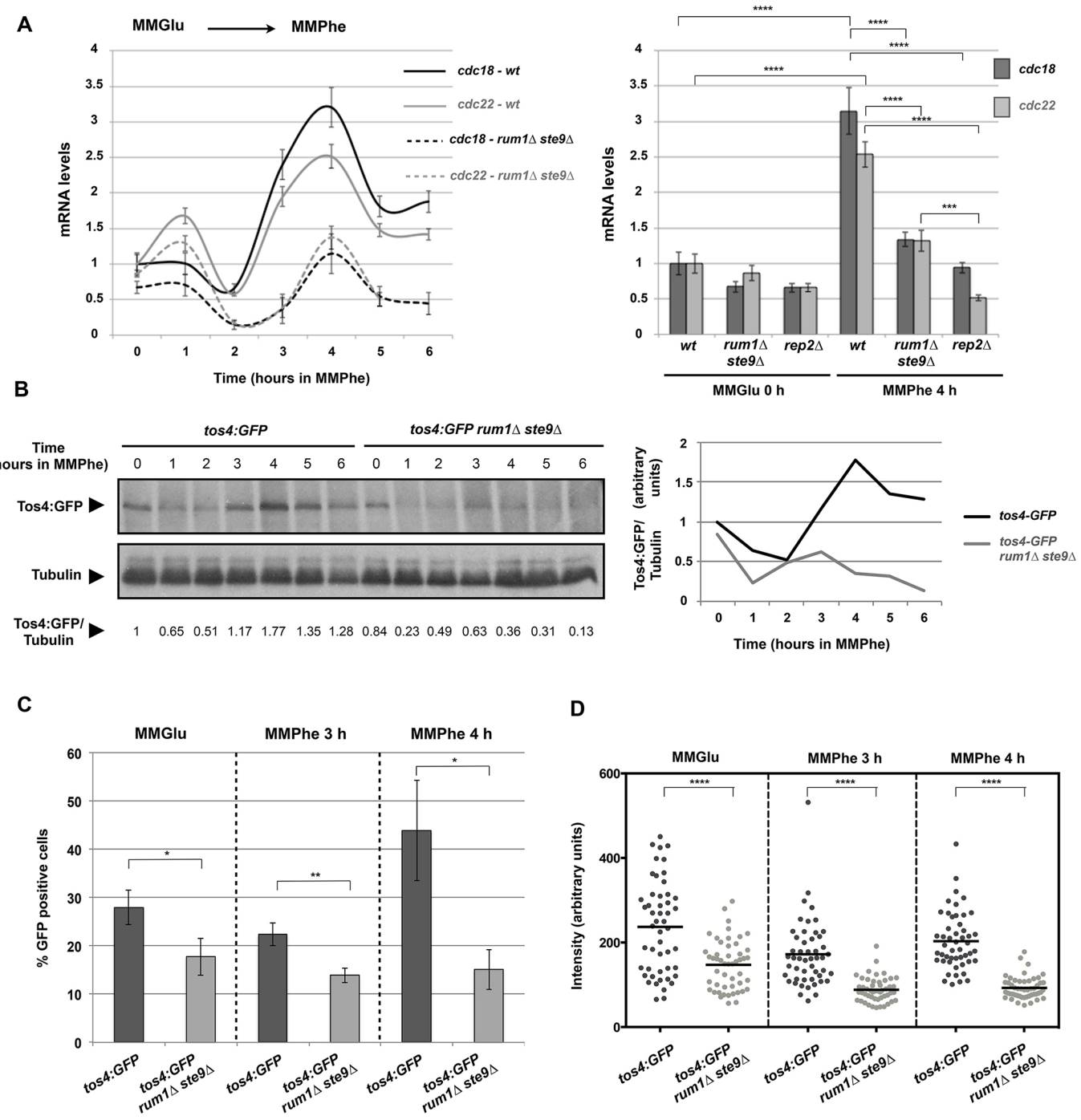

Fig. 7. MBF-dependent transcription is downregulated in cells lacking Rum1 and Ste9. (A) Wild-type (wt), *rum1Δ ste9Δ* and *rep2Δ* mutant cells were grown in MMGlu and then shifted to MMPhe. Samples of cells to isolate RNA were taken at 0, 1, 2, 3, 4, 5 and 6 h after the shift. (A) Levels of *cdc18*$^{+}$ and *cdc22*$^{+}$ mRNA were determined by RT-qPCR. The RNA levels were first normalized against the constitutively expressed actin gene, following the normalization against the wt strain grown in MMGlu. (B) *tos4:GFP* and *tos4:GFP rum1Δ ste9Δ* cells were shifted from MMGlu to MMPhe. Western blot using anti-GFP antibodies was used to determine the levels of Tos4:GFP at the indicated times after the shift from MMGlu to MMPhe. Tubulin was used as a protein loading control. The ratio of Tos4:GFP to tubulin was determined for each sample (left panel). Graphic representation of the Tos4:GFP to tubulin ratios at different time points (right panel). (C) Percentage of Tos4:GFP-positive cells in wt and in *rum1Δ ste9Δ* mutant cells in MMGlu and 3 and 4 h after the shift to MMPhe. (D) Intensity of the Tos4:GFP signal in the wt and in the *rum1Δ ste9Δ* mutant in MMGlu and 3 and 4 h after the shift to MMPhe. *P<0.01, **P<0.001, ***P<0.0001, ****P<0.00001.

(Fig. S7A), suggesting suppression of the *rum1Δ ste9Δ* phenotype by deleting *nrm1*$^{+}$. The triple mutant *nrm1Δ rum1Δ ste9Δ* presented a phenotype similar to that of *nrm1Δ* cells, with less Rad52:YFP nuclear foci than *rum1Δ ste9Δ* cells in MMPhe (Fig. S7B). Deletion of *nrm1*$^{+}$ also rescued the growth defect phenotype of the *rum1Δ ste9Δ* in MMPhe (Fig. S4). Flow cytometry analysis revealed that the S phase population present in *rum1Δ ste9Δ* cells in MMPhe was not detected in *nrm1Δ rum1Δ ste9Δ*, probably due to the long G2 phase of the *nrm1Δ* mutant (Fig. S7C, arrowhead). These results are consistent with the idea that deletion of *rum1*$^{+}$ and *ste9*$^{+}$ causes DNA replication stress in nitrogen-poor media because of downregulation of MBF activity. It is possible that deletion of

Journal of Cell Science (2018) 131, jcs218743. doi:10.1242/jcs.218743

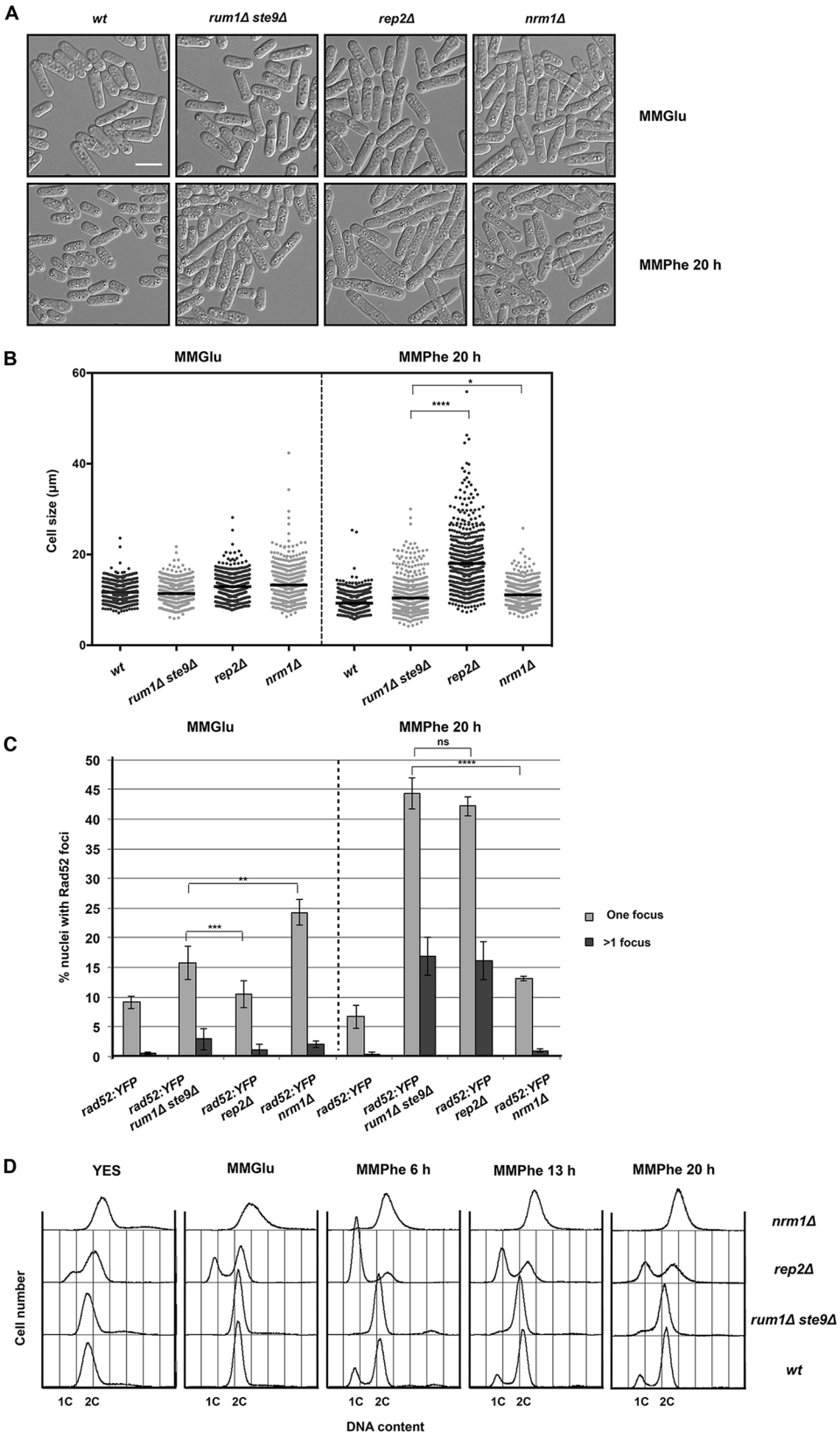

Fig. 8. Reduced MBF activity promotes DNA damage in nitrogen-poor medium. Wild-type (wt), *rum1Δ ste9Δ*, *rep2Δ* (downregulated MBF) and *nrm1Δ* (upregulated MBF) cells were grown in MMGlu and then shifted to MMPhe for 20 h. (A) DIC microscopy images of live cells after 20 h in MMPhe. Scale bar: 10 µM. (B) Cell lengths of 600 cells stained with blankophor growing in MMGlu or in MMPhe for 20 h. The bar represents the average value. (C) Percentage±s.d. of cells with one (light grey) or more than one (dark grey) Rad52:YFP nuclear foci in MMGlu and after 20 h of growth in MMPhe. Three experimental replicas were counted at each time point (n=500 cells per replica and time point). (D) FACS profile showing the DNA content (1C and 2C) of wt, *rum1Δ ste9Δ*, *rep2Δ* and *nrm1Δ* mutant cells in YES, MMGlu and 6, 13 and 20 h after the shift to MMPhe. *P<0.01, **P<0.001, ***P<0.0001, ****P<0.00001.

nrm1^{+} rescues the phenotype of the *rum1Δ ste9Δ* mutant cells by increasing MBF activity or by extending the G2 phase, which allows more time for DNA repair, similar to what happens to *cdc2-asM17 rum1Δ ste9Δ* cells or when the *rum1Δ ste9Δ* mutant cells are grown in nitrogen-rich medium.

DISCUSSION

Here, we show that inhibition of Cdk1 activity in G1 by Rum1 and Ste9 is required in order to promote a proper wave of MBF-dependent transcription at the G1/S boundary, which is necessary for an efficient S phase. This function of Ste9 and Rum1 is particularly important in

Journal of Cell Science (2018) 131, jcs218743. doi:10.1242/jcs.218743

cells growing in nitrogen-poor media, where the G1 phase of the cell cycle has to be extended before cells can undergo DNA replication. Consistent with this idea, cells lacking Rum1 and Ste9 enter prematurely into S phase with significantly reduced expression of *cdc18*$^{+}$, *cdc22*$^{+}$ and *tos4*$^{+}$ MBF targets.

Cdk1 protein kinase activity is high in mitosis, drops during anaphase and G1, rises again at the end of G1 to promote S phase and keeps increasing during G2 until the onset of mitosis (Coudreuse and Nurse, 2010). This oscillatory behaviour of Cdk1 activity is important for the periodic expression of cell cycle genes in fission yeast (Banyai et al., 2016). APC/C–Ste9-dependent degradation of Cdc13 and Rum1 inhibition of the Cdk1 kinase generate a window of low Cdk1 activity in G1 that it is crucial in fission yeast cells growing in nitrogen-poor medium, where the G1 phase of the cell cycle has to be extended. We also show that Rum1 and Ste9 are upregulated in nitrogen-poor media and that they are required to prevent genomic instability in subsequent cell cycles. In nitrogen-rich media, there is no apparent defect of the *rum1*$^{+}$ and *ste9*$^{+}$ deletions, although the double mutant shows mild hydroxyurea sensitivity. However, when *rum1Δ ste9Δ* mutant cells are grown in nitrogen-poor medium, they show a slow S phase, high levels of DNA damage and cell cycle delay in G2 promoted by activation of the DNA damage checkpoint. This phenotype is rescued by extending the G2 phase in cells with reduced CDK activity (*cdc2-asM17*, a hypomorph allele of *cdc2*$^{+}$) or aggravated by reducing the G2 phase in cells with reduced PP2A activity (*ppa2Δ*, lacking one of the two catalytic subunits of PP2A).

At the onset of S phase, Cdk1 activates the MBF transcription factor (Banyai et al., 2016; Reymond et al., 1993), the fission yeast functional orthologue of mammalian E2F, which promotes the expression of genes involved in nucleotide biogenesis, S phase progression and DNA repair (Bähler, 2005). The MBF complex is bound to its target promoters throughout the cell cycle and it is tightly regulated by positive and negative factors that restrict MBF activation to the G1/S transition (Wuarin et al., 2002). Rep2 is an MBF transcriptional activator, whereas Nrm1 and Yox1 are transcriptional repressors of MBF during S phase and G2 (Baum et al., 1997; Aligianni et al., 2009; Nakashima et al., 1995; de Bruin et al., 2006). Although it has been described that mutant cells with increased MBF activity (*yox1Δ* or *nrm1Δ*) present genomic instability when they are cultured under standard laboratory conditions (nitrogen-rich media) (Caetano et al., 2014; Gómez-Escoda et al., 2011), here, we show that upregulation of MBF is less detrimental in nitrogen-poor medium (MMPhe). In fact, reduction of MBF activity in *rep2Δ* and in *rum1Δ ste9Δ* mutants cells generated high levels of DNA damage in nitrogen-poor medium (MMPhe), supporting the idea that, in nitrogen-poor conditions, higher levels of MBF-dependent transcription activity are required at the end of G1 for an efficient S phase. Moreover, deletion of *nrm1*$^{+}$, which upregulates MBF activity, partially rescued the genomic instability of *rum1Δ ste9Δ* cells in MMPhe.

Our findings are in agreement with recent results reporting that loss of the Set2 histone H3 lysine 36 (H3K36) methyl transferase generates reduced MBF-dependent ribonucleotide reductase (*cdc22*$^{+}$) expression, causing a drop in the dNTP pools, abnormal replication origin firing, S phase delay and genotoxic stress (Pai et al., 2017). As in the *rum1Δ ste9Δ* mutant, the delay in S phase and the replication stress can be supressed in *set2Δ* cells by increasing the dNTP levels by deleting the MBF repressor *nrm1*$^{+}$ (our work) or *yox1*$^{+}$ (Pai et al., 2017) or the RNR inhibitor *spd1*$^{+}$ (Liu et al., 2003; Håkansson et al., 2006).

Sic1, the budding yeast orthologue of Rum1, is stabilised in G1 in nitrogen-poor media (Moreno-Torres et al., 2015). Sic1 promotes origin licensing during G1 by inhibiting CDK activity (Lengronne and Schwob, 2002; Tanaka and Diffley, 2002). Furthermore, Cdh1 (the budding yeast orthologue of Ste9) together with Sic1 is required to prevent chromosome instability by promoting efficient origin firing (Ayuda-Durán et al., 2014). In animal cells, acute depletion or permanent ablation of Cdh1 causes genomic instability in primary mouse embryonic fibroblasts by slowing down DNA replication fork movement and increasing origin activity (García-Higuera et al., 2008; Garzón et al., 2017). Moreover, aberrant activation of the Rb–E2F pathway, which is very common in many cancers, leads to overexpression of cyclin E, depletion of the dNTP pool and inefficient DNA replication (Bester et al., 2011). In these cells, DNA replication dynamics are altered and S phase takes longer as a result of reduced licensing and increased origin firing (Jones et al., 2013). However, there is no published evidence, either for budding yeast or animal cells, of the connection between CDK inhibition in G1 and G1/S transcription. In the future, it is important to establish whether this connection is also conserved in all eukaryotic cells and whether reduced MBF/E2F activity also generates DNA replication stress, considering that Cdk1 regulation, MBF/E2F-dependent transcription and S phase activation are highly conserved processes.

In summary, we have found that the cell cycle inhibitor Rum1 and the APC/C co-activator Ste9 are upregulated in nitrogen-poor medium. These two proteins are required to inhibit Cdk1 activity in G1, which delays the G1/S transition and facilitates efficient DNA replication by regulating the amplitude of MBF activity. In nitrogen-poor medium, proper levels of MBF-dependent transcription are necessary to generate an optimal S phase.

MATERIALS AND METHODS

Fission yeast strains and methods

The fission yeast strains used in this study are listed in Table S1. Fission yeast cells were grown and manipulated genetically according to standard protocols (Moreno et al., 1991). Genetic crosses were performed on malt extract agar plates. All the strains containing *rum1*$^{+}$ and *ste9*$^{+}$ deletions were obtained by direct transformations, because of the sterility of both deletions, using a PCR-based strategy (Bähler et al., 1998). Oligonucleotides with 80 bases of homology to regions before the initiation codon and after the stop codon were used to amplify the kanMX6, natMX6 or hphMX6 marker sequences from plasmids pFA6a-kanMX6/natMX6/pFA6a-hphMX6. The PCR product was used to transform a given strain.

Cells were grown overnight at 32°C in yeast extract supplemented with adenine, leucine, histidine, lysine and uracil (YES) and then transferred to Edinburgh minimal medium containing 20 mM glutamate (MMGlu) instead of 5 g l^{-1} NH_4Cl, as a nitrogen source. MMGlu is considered a nitrogen-rich medium. The generation time of wild-type cells in MMGlu at 32°C is 2.5 h. Cells grown in MMGlu for 1 day were transferred to minimal medium containing 20 mM phenylalanine (MMPhe) or to minimal medium without nitrogen (MM-N). MMPhe is considered a nitrogen-poor medium. The generation time of wild-type cells in MMPhe at 32°C is 6 h. In all cases, cells grown to mid-exponential phase (5×10^{6}–8×10^{6} cells ml^{-1}) were centrifuged and washed in the destination medium. For hydroxyurea (HU) sensitivity experiments, HU (Sigma-Aldrich) was added to YES plates from a 1 M stock solution at a final concentration of 5 or 6 mM. All experiments were performed with prototrophic strains to avoid the addition of supplements (amino acids or uracil, which could be used as a nitrogen source) to the minimal medium.

Microscopy

For cell size measurements and Tos4:GFP detection, 2×10^{6} exponentially growing cells were washed in phosphate-buffered saline (PBS) and resuspended in 3.5 µl of 50 µg ml^{-1} Blankophor (Bayer) and examined under a Nikon Eclipse 90i fluorescence microscope equipped with a Plan/

Apo 603 oil objective lens and a Hamamatsu ORCA-ER camera. Live images were acquired with MetaMorph software (Molecular Devices). Cell length was measured from pictures of 600 cells. Tos4:GFP-positive cells were quantified from 500 cells in three independent experiments. The Tos4:GFP intensity signal was obtained from 50 cells using ImageJ (NIH).

For Rad52:YFP nuclear foci detection, 500 µl of cells growing in exponential phase in MMGlu or MMPhe were collected and Rad52:YFP foci were visualized using a DeltaVision microscope and SoftWoRx Resolve 3D software (Applied Precision). The percentages were measured from maximum-intensity projections of 12 0.3 µm z-sections (Image J, NIH) of 500 nuclei. Rad52:YFP nuclear foci were represented as the mean of nuclei with Rad52:YFP foci, with the standard deviation from three independent experiments.

For the detection of aberrant mitosis, samples of 2×10^6 cells fixed in 70% (v/v) ethanol were washed in PBS and resuspended in 2.6 µl of 1 µg ml^{-1} 4′,6-diamidino-2-phenylindole (DAPI) and 1.1 µl of 50 µg ml^{-1} Blankophor (Bayer) and examined under a Leica DM XRA or Nikon Eclipse 90i fluorescence microscope equipped with a Hamamatsu ORCA-ER camera. The percentage of aberrant mitosis was determined from pictures of 950–1000 cells using ImageJ (NIH).

BrdU immunofluorescence

BrdU incorporation was performed using the *h*$^+$ *ura4-D18::P3nmt1-Tk-ura4*$^+$ strain and following the immunofluorescence protocol (Hodson et al., 2003) with modifications. Cells were labelled for 20 min in MMGlu or MMPhe without thiamine containing 2.5 µM BrdU (Becton-Dickinson) at 32°C. DNA denaturation was performed in 1 ml of 2 M HCl, 0.1% Triton X-100 and incubated for 30 min. Cells were neutralized with 0.1 M sodium tetraborate, pH 9. BrdU-positive cells were counted in pictures of 900 nuclei (Image J, NIH).

Protein methods

Protein extracts were obtained using trichloroacetic acid extraction (Foiani et al., 1994). For western blot analysis, anti-Rum1 (1:250; Benito et al., 1998), anti-Ste9 (1:200; Blanco et al., 2000), anti-HA (1:500; 12CA5, Roche), anti-GFP (1:1500; A11122, Molecular Probes) and anti-tubulin (1:10,000; a gift from Dr Keith Gull, University of Oxford, UK) antibodies were used. The secondary antibodies were HRP-conjugated anti-mouse IgG (1:2500; NA-931, Amersham) and anti-rabbit IgG (1:3000; NA-934, Amersham). Detection was performed using the enhanced chemiluminescence procedure (ECL kit).

RNA extraction and RT-qPCR

Total RNA was isolated from 1×10^8 cells from exponential phase using an RNeasy Mini Kit (Qiagen) as described by the manufacturer. cDNA synthesis was performed with the SuperScript II First-Strand Synthesis System (Invitrogen) in a final volume of 50 µl using 3 µg of RNA previously treated with DNAse I (Invitrogen). cDNA (1 µl) was then used for the quantitative reactions in an Applied Biosystems 7300 Real-Time PCR System. For each reaction, the SYBR *Premix Ex Taq* (TaKaRa) reagent was used with oligonucleotide concentrations of 0.2 µM. Specific oligonucleotides were as follows: forward 5′-ACACACTCAAGATGT-GTGCTATGAT-3′ and reverse 5′-CATTAGTTCCAGCAATATACGAA-CC for *cdc22*$^+$; forward 5′-TAAATTACCCACAACACCTCAAACT-3′ and reverse 5′-ATGGAACAGGATTACATGTACGATT-3′ for *cdc18*$^+$; and forward 5′-CCTTGCTTGTTGACTGAGGCTC-3′ and reverse 5′-GCAACATAAAAGGCAGGTGCAT-3′ for the actin gene. The thermal cycling conditions were as follows: 95°C for 45 s, 40 cycles of 95°C for 5 s and 60°C for 31 s, followed by a dissociation step at 95°C for 15 s, 60°C for 1 min and 95°C for 15 s. Reactions were run in triplicate and negative controls without reverse transcriptase or cDNA were included in each run. Determination of the PCR efficiency was performed from serial dilutions of wild-type *S. pombe* genomic DNA (1:10, 1:100, 1:1000, 1:10,000, 1:100,000) to generate a standard curve for each reaction. Expression ratios were calculated according to the mathematic model described by Pfaffl (2001). The samples were first normalized against the constitutively expressed actin gene, following normalization against the wild-type strain grown in MMGlu. The experiments were performed at least twice with cDNA from different biological repeats.

Statistical analysis

Column graphs show mean±s.d. Two-tailed Student's *t*-tests were used to calculate significant differences between two groups and one-way ANOVA between more than two groups; the Prism 6 software (GraphPad) was used. A *P* value of 0.05 or lower was regarded as statistically significant.

Acknowledgements

We thank all members of the S.M. laboratory, University of Salamanca for helpful discussions. We are grateful to J. Ayté, T. Carr, R. Daga, H. Masukata and M. Sato for strains.

Competing interests

The authors declare no competing or financial interests.

Author contributions

Conceptualization: A.R., N.G.-B., S.M.; Methodology: A.R., N.G.-B., A.V.-B., M.S., S.M.; Software: A.V.-B., M.S.; Validation: A.R., N.G.-B., A.V.-B., M.S.; Formal analysis: A.R., N.G.-B., A.V.-B., M.S.; Investigation: A.R., N.G.-B., A.V.-B., M.S.; Resources: N.G.-B., S.M.; Data curation: A.R., N.G.-B., S.M.; Writing - original draft: A.R., S.M.; Writing - review & editing: A.R., N.G.-B., A.V.-B., M.S., S.M.; Visualization: A.R., N.G.-B., S.M.; Supervision: S.M.; Project administration: S.M.; Funding acquisition: S.M.

Funding

This research was funded by grants from the Ministerio de Economía y Competitividad (BFU2011-28274, BFU2014-55439-R and BFU2017-88335-R) and the Junta de Castilla y León (CSI084U16). A.R. and A.V.-B. were recipients of FPI pre-doctoral training grants and N.G.-B. received an FPU pre-doctoral training grant.

Supplementary information

Supplementary information available online at
http://jcs.biologists.org/lookup/doi/10.1242/jcs.218743.supplemental

References

Aligianni, S., Lackner, D. H., Klier, S., Rustici, G., Wilhelm, B. T., Marguerat, S., Codlin, S., Brazma, A., de Bruin, R. A. M. and Bähler, J. (2009). The fission yeast homeodomain protein Yox1p binds to MBF and confines MBF-dependent cell-cycle transcription to G1-S via negative feedback. *PLoS Genet.* **5**, e1000626.

Aoi, Y., Kawashima, S. A., Simanis, V., Yamamoto, M. and Sato, M. (2014). Optimization of the analogue-sensitive Cdc2/Cdk1 mutant by in vivo selection eliminates physiological limitations to its use in cell cycle analysis. *Open Biol.* **4**, 140063-140063.

Ayté, J., Leis, J. F., Herrera, A., Tang, E., Yang, H. and DeCaprio, J. A. (1995). The *Schizosaccharomyces pombe* MBF complex requires heterodimerization for entry into S phase. *Mol. Cell. Biol.* **15**, 2589-2599.

Ayté, J., Schweitzer, C., Zarzov, P., Nurse, P. and DeCaprio, J. A. (2001). Feedback regulation of the MBF transcription factor by cyclin Cig2. *Nat. Cell. Biol.* **3**, 1043-1050.

Ayuda-Durán, P., Devesa, F., Gomes, F., Sequeira-Mendes, J., Avila-Zarza, C., Gómez, M. and Calzada, A. (2014). The CDK regulators Cdh1 and Sic1 promote efficient usage of DNA replication origins to prevent chromosomal instability at a chromosome arm. *Nucleic Acids Res.* **42**, 7057-7068.

Bähler, J. (2005). Cell-cycle control of gene expression in budding and fission yeast. *Annu. Rev. Genet.* **39**, 69-94.

Bähler, J., Wu, J.-Q., Longtine, M. S., Shah, N. G., Mckenzie, A., Ill, Steever, A. B., Wach, A., Philippsen, P. and Pringle, J. R. (1998). Heterologous modules for efficient and versatile PCR-based gene targeting in *Schizosaccharomyces pombe*. *Yeast* **14**, 943-951.

Banyai, G., Baïdi, F., Coudreuse, D. and Szilagyi, Z. (2016). Cdk1 activity acts as a quantitative platform for coordinating cell cycle progression with periodic transcription. *Nat. Commun.* **7**, 11161.

Baum, B., Wuarin, J. and Nurse, P. (1997). Control of S-phase periodic transcription in the fission yeast mitotic cycle. *EMBO J.* **16**, 4676-4688.

Benito, J., Martín-Castellanos, C. and Moreno, S. (1998). Regulation of the G1 phase of the cell cycle by periodic stabilization and degradation of the p25^{rum1} CDK inhibitor. *EMBO J.* **17**, 482-497.

Bester, A. C., Roniger, M., Oren, Y. S., Im, M. M., Sarni, D., Chaoat, M., Bensimon, A., Zamir, G., Shewach, D. S. and Kerem, B. (2011). Nucleotide deficiency promotes genomic instability in early stages of cancer development. *Cell* **145**, 435-446.

Blanco, M. A., Sánchez-Díaz, A., de Prada, J. M. and Moreno, S. (2000). APC$^{ste9/srw1}$ promotes degradation of mitotic cyclins in G1 and is inhibited by cdc2 phosphorylation. *EMBO J.* **19**, 3945-3955.

Brondello, J.-M., Boddy, M. N., Furnari, B. and Russell, P. (1999). Basis for the checkpoint signal specificity that regulates Chk1 and Cds1 protein kinases. *Mol. Cell. Biol.* **19**, 4262-4269.

Caetano, C., Klier, S. and de Bruin, R. A. M. (2011). Phosphorylation of the MBF repressor Yox1p by the DNA replication checkpoint keeps the G1/S cell-cycle transcriptional program active. *PLoS ONE* **6**, e17211.
Caetano, C., Limbo, O., Farmer, S., Klier, S., Dovey, C., Russell, P. and de Bruin, R. A. M. (2014). Tolerance of deregulated G1/S transcription depends on critical G1/S regulon genes to prevent catastrophic genome instability. *Cell Rep.* **9**, 2279-2289.
Capasso, H., Palermo, C., Wan, S., Rao, H., John, U. P., O'Connell, M. J. and Walworth, N. C. (2002). Phosphorylation activates Chk1 and is required for checkpoint-mediated cell cycle arrest. *J. Cell Sci.* **115**, 4555-4564.
Carlson, C. R., Grallert, B., Stokke, T. and Boye, E. (1999). Regulation of the start of DNA replication in *Schizosaccharomyces pombe*. *J. Cell Sci.* **112**, 939-946.
Caspari, T. and Carr, A. M. (1999). DNA structure checkpoint pathways in *Schizosaccharomyces pombe*. *Biochimie* **81**, 173-181.
Chabes, A. and Stillman, B. (2007). Constitutively high dNTP concentration inhibits cell cycle progression and the DNA damage checkpoint in yeast *Saccharomyces cerevisiae*. *Proc. Natl. Acad. Sci. USA* **104**, 1183-1188.
Chica, N., Rozalén, A. E., Pérez-Hidalgo, L., Rubio, A., Novak, B. and Moreno, S. (2016). Nutritional control of cell size by the Greatwall-Endosulfine-PP2A·B55 pathway. *Curr. Biol.* **26**, 319-330.
Correa-Bordes, J., Gulli, M. P. and Nurse, P. (1997). $p25^{rum1}$ promotes proteolysis of the mitotic B-cyclin $p56^{cdc13}$ during G1 of the fission yeast cell cycle. *EMBO J.* **16**, 4657-4664.
Coudreuse, D. and Nurse, P. (2010). Driving the cell cycle with a minimal CDK control network. *Nature* **468**, 1074-1079.
Daga, R. R., Bolaños, P. and Moreno, S. (2003). Regulated mRNA stability of the Cdk inhibitor Rum1 links nutrient status to cell cycle progression. *Curr. Biol.* **13**, 2015-2024.
de Bruin, R. A. M., Kalashnikova, T. I., Chahwan, C., McDonald, W. H., Wohlschlegel, J., Yates, J., Russell, P. and Wittenberg, C. (2006). Constraining G1-specific transcription to late G1 phase: the MBF-associated corepressor Nrm1 acts via negative feedback. *Mol. Cell* **23**, 483-496.
de Bruin, R. A. M., Kalashnikova, T. I., Aslanian, A., Wohlschlegel, J., Chahwan, C., Yates, J. R., Russell, P. and Wittenberg, C. (2008). DNA replication checkpoint promotes G1-S transcription by inactivating the MBF repressor Nrm1. *Proc. Natl. Acad. Sci. USA* **105**, 11230-11235.
Fantes, P. and Nurse, P. (1977). Control of cell size at division in fission yeast by a growth-modulated size control over nuclear division. *Exp. Cell Res.* **107**, 377-386.
Fernández-Sarabia, M. J., McInerny, C., Harris, P., Gordon, C. and Fantes, P. (1993). The cell cycle genes $cdc22^{+}$ and $suc22^{+}$ of the fission yeast *Schizosaccharomyces pombe* encode the large and small subunits of ribonucleotide reductase. *Mol. Gen. Genet.* **238**, 241-251.
Fleck, O., Vejrup-Hansen, R., Watson, A., Carr, A. M., Nielsen, O. and Holmberg, C. (2013). Spd1 accumulation causes genome instability independently of ribonucleotide reductase activity but functions to protect the genome when deoxynucleotide pools are elevated. *J. Cell Sci.* **126**, 4985-4994.
Foiani, M., Marini, F., Gamba, D., Lucchini, G. and Plevani, P. (1994). The B subunit of the DNA polymerase alpha-primase complex in *Saccharomyces cerevisiae* executes an essential function at the initial stage of DNA replication. *Mol. Cell. Biol.* **14**, 923-933.
García-Higuera, I., Manchado, E., Dubus, P., Cañamero, M., Méndez, J., Moreno, S. and Malumbres, M. (2008). Genomic stability and tumour suppression by the APC/C cofactor Cdh1. *Nat. Cell Biol.* **10**, 802-811.
Garzón, J., Rodríguez, R., Kong, Z., Chabes, A., Rodríguez-Acebes, S., Méndez, J., Moreno, S. and García-Higuera, I. (2017). Shortage of dNTPs underlies altered replication dynamics and DNA breakage in the absence of the APC/C cofactor Cdh1. *Oncogene* **36**, 5808-5818.
Gaspa, L., González-Medina, A., Hidalgo, E. and Ayté, J. (2016). A functional genome-wide genetic screening identifies new pathways controlling the G1/S transcriptional wave. *Cell Cycle* **15**, 720-729.
Gómez-Escoda, B., Ivanova, T., Calvo, I. A., Alves-Rodrigues, I., Hidalgo, E. and Ayté, J. (2011). Yox1 links MBF-dependent transcription to completion of DNA synthesis. *EMBO Rep.* **12**, 84-89.
Håkansson, P., Dahl, L., Chilkova, O., Domkin, V. and Thelander, L. (2006). The *Schizosaccharomyces pombe* replication inhibitor Spd1 regulates ribonucleotide reductase activity and dNTPs by binding to the large Cdc22 subunit. *J. Biol. Chem.* **281**, 1778-1783.
Hodson, J. A., Bailis, J. M. and Forsburg, S. L. (2003). Efficient labeling of fission yeast *Schizosaccharomyces pombe* with thymidine and BUdR. *Nucleic Acids Res.* **31**, e134.
Hofmann, J. F. and Beach, D. (1994). Cdt1 is an essential target of the Cdc10/Sct1 transcription factor: requirement for DNA replication and inhibition of mitosis. *EMBO J.* **13**, 425-434.
Holmberg, C., Fleck, O., Hansen, H. A., Liu, C., Slaaby, R., Carr, A. M. and Nielsen, O. (2005). Ddb1 controls genome stability and meiosis in fission yeast. *Genes Dev.* **19**, 853-862.
Ivanova, T., Gómez-Escoda, B., Hidalgo, E. and Ayté, J. (2011). G1/S transcription and the DNA synthesis checkpoint: common regulatory mechanisms. *Cell Cycle* **10**, 912-915.
Jones, R. M., Mortusewicz, O., Afzal, I., Lorvellec, M., García, P., Helleday, T. and Petermann, E. (2013). Increased replication initiation and conflicts with transcription underlie Cyclin E-induced replication stress. *Oncogene* **32**, 3744-3753.
Kelly, T. J., Martin, G. S., Forsburg, S. L., Stephen, R. J., Russo, A. and Nurse, P. (1993). The fission yeast $cdc18^{+}$ gene product couples S phase to START and mitosis. *Cell* **74**, 371-382.
Kiang, L., Heichinger, C., Watt, S., Bähler, J. and Nurse, P. (2009). Cyclin-dependent kinase inhibits reinitiation of a normal S-phase program during G2 in fission yeast. *Mol. Cell. Biol.* **29**, 4025-4032.
Kim, W. J., Lee, S., Park, M. S., Jang, Y. K., Kim, J. B. and Park, S. D. (2000). Rad22 protein, a Rad52 homologue in *Schizosaccharomyces pombe*, binds to DNA double-strand breaks. *J. Biol. Chem.* **275**, 35607-35611.
Kinoshita, N., Yamano, H., Niwa, H., Yoshida, T. and Yanagida, M. (1993). Negative regulation of mitosis by the fission yeast protein phosphatase ppa2. *Genes Dev.* **7**, 1059-1071.
Kitamura, K., Maekawa, H. and Shimoda, C. (1998). Fission yeast Ste9, a homolog of Hct1/Cdh1 and Fizzy-related, is a novel negative regulator of cell cycle progression during G1-phase. *Mol. Biol. Cell* **9**, 1065-1080.
Kominami, K.-I., Seth-Smith, H. and Toda, T. (1998). Apc10 and Ste9/Srw1, two regulators of the APC–cyclosome, as well as the CDK inhibitor Rum1 are required for G1 cell-cycle arrest in fission yeast. *EMBO J.* **17**, 5388-5399.
Lengronne, A. and Schwob, E. (2002). The yeast CDK inhibitor Sic1 prevents genomic instability by promoting replication origin licensing in late G1. *Mol. Cell.* **9**, 1067-1078.
Lindsay, H. D., Griffiths, D. J. F., Edwards, R. J., Christensen, P. U., Murray, J. M., Osman, F., Walworth, N. C. and Carr, A. M. (1998). S-phase-specific activation of Cds1 kinase defines a subpathway of the checkpoint response in *Schizosaccharomyces pombe*. *Genes Dev.* **12**, 382-395.
Liu, C., Powell, K. A., Mundt, K., Wu, L., Carr, A. M. and Caspari, T. (2003). Cop9/signalosome subunits and Pcu4 regulate ribonucleotide reductase by both checkpoint-dependent and -independent mechanisms. *Genes Dev.* **17**, 1130-1140.
Liu, C., Poitelea, M., Watson, A., Yoshida, S.-I., Shimoda, C., Holmberg, C., Nielsen, O. and Carr, A. M. (2005). Transactivation of *Schizosaccharomyces pombe* $cdt2^{+}$ stimulates a Pcu4-Ddb1-CSN ubiquitin ligase. *EMBO J.* **24**, 3940-3951.
Lowndes, N. F., McInerny, C. J., Johnson, A. L., Fantes, P. A. and Johnston, L. H. (1992). Control of DNA synthesis genes in fission yeast by the cell-cycle gene $cdc10^{+}$. *Nature* **355**, 449-453.
Maqbool, Z., Kersey, P. J., Fantes, P. A. and McInerny, C. J. (2003). MCB-mediated regulation of cell cycle-specific $cdc22^{+}$ transcription in fission yeast. *Mol. Genet. Genomics* **269**, 765-775.
Martín-Castellanos, C., Blanco, M. A., de Prada, J. M. and Moreno, S. (2000). The puc1 cyclin regulates the G1 phase of the fission yeast cell cycle in response to cell size. *Mol. Biol. Cell* **11**, 543-554.
Meister, P., Taddei, A., Vernis, L., Poidevin, M., Gasser, S. M. and Baldacci, G. (2005). Temporal separation of replication and recombination requires the intra-S checkpoint. *J. Cell Biol.* **168**, 537-544.
Moreno, S. and Nurse, P. (1994). Regulation of progression through the G1 phase of the cell cycle by the *rum1+* gene. *Nature* **367**, 236-242.
Moreno, S., Klar, A. and Nurse, P. (1991). Molecular genetic analysis of fission yeast *Schizosaccharomyces pombe*. *Methods Enzymol.* **194**, 795-823.
Moreno-Torres, M., Jaquenoud, M. and De Virgilio, C. (2015). TORC1 controls G1-S cell cycle transition in yeast via Mpk1 and the greatwall kinase pathway. *Nat. Commun.* **6**, 8256.
Nakashima, N., Tanaka, K., Sturm, S. and Okayama, H. (1995). Fission yeast Rep2 is a putative transcriptional activator subunit for the cell cycle "start" function of Res2-Cdc10. *EMBO J.* **14**, 4794-4802.
Nasmyth, K., Nurse, P. and Fraser, R. S. (1979). The effect of cell mass on the cell cycle timing and duration of S-phase in fission yeast. *J. Cell Sci.* **39**, 215-233.
Navarro, F. J. and Nurse, P. (2012). A systematic screen reveals new elements acting at the G2/M cell cycle control. *Genome Biol.* **13**, R36.
Nurse, P. (1975). Genetic control of cell size at cell division in yeast. *Nature* **256**, 547-551.
Nurse, P. and Thuriaux, P. (1977). Controls over the timing of DNA replication during the cell cycle of fission yeast. *Exp. Cell Res.* **107**, 365-375.
Nurse, P., Thuriaux, P. and Nasmyth, K. (1976). Genetic control of the cell division cycle in the fission yeast *Schizosaccharomyces pombe*. *Mol. Gen. Genet.* **146**, 167-178.
Pai, C.-C., Kishkevich, A., Deegan, R. S., Keszthelyi, A., Folkes, L., Kearsey, S. E., De León, N., Soriano, I., de Bruin, R. A. M., Carr, A. M. et al. (2017). Set2 methyltransferase facilitates DNA replication and promotes genotoxic stress responses through MBF-dependent transcription. *Cell Rep.* **20**, 2693-2705.
Pérez-Hidalgo, L. and Moreno, S. (2017). Coupling TOR to the cell cycle by the Greatwall–Endosulfine–PP2A-B55 pathway. *Biomolecules* **7**, 59.
Petersen, J. and Nurse, P. (2007). TOR signalling regulates mitotic commitment through the stress MAP kinase pathway and the Polo and Cdc2 kinases. *Nat. Cell. Biol.* **9**, 1263-1272.

Pfaffl, M. W. (2001). A new mathematical model for relative quantification in real-time RT–PCR. *Nucleic Acids Res.* **29**, e45.
Pfister, S. X., Markkanen, E., Jiang, Y., Sarkar, S., Woodcock, M., Orlando, G., Mavrommati, I., Pai, C.-C., Zalmas, L.-P., Drobnitzky, N. et al. (2015). Inhibiting Wee1 selectively kills histone H3K36me3-deficient cancers by dNTP starvation. *Cancer Cell* **28**, 557-568.
Purtill, F. S., Whitehall, S. K., Williams, E. S., McInerny, C. J., Sharrocks, A. D. and Morgan, B. A. (2011). A homeodomain transcription factor regulates the DNA replication checkpoint in yeast. *Cell Cycle* **10**, 664-670.
Reymond, A., Marks, J. and Simanis, V. (1993). The activity of *S. pombe* DSC-1 -like factor is cell cycle regulated and dependent on the activity of $p34^{cdc2}$. *EMBO J.* **12**, 4325-4334.
Rhind, N. and Russell, P. (1998). Mitotic DNA damage and replication checkpoints in yeast. *Curr. Opin. Cell Biol.* **10**, 749-758.
Stern, B. and Nurse, P. (1998). Cyclin B proteolysis and the cyclin-dependent kinase inhibitor Rum1p are required for pheromone-induced G1 arrest in fission yeast. *Mol. Biol. Cell* **9**, 1309-1321.
Stillman, B. (2013). Deoxynucleoside triphosphate (dNTP) synthesis and destruction regulate the replication of both cell and virus genomes. *Proc. Natl. Acad. Sci. USA* **110**, 14120-14121.
Sveiczer, A., Novak, B. and Mitchison, J. M. (1996). The size control of fission yeast revisited. *J. Cell Sci.* **109**, 2947-2957.
Tahara, S., Tanaka, K., Yuasa, Y. and Okayama, H. (1998). Functional domains of Rep2, a transcriptional activator subunit for Res2-Cdc10, controlling the cell cycle “start”. *Mol. Biol. Cell* **9**, 1577-1588.
Tanaka, S. and Diffley, J. F. X. (2002). Deregulated G1-cyclin expression induces genomic instability by preventing efficient pre-RC formation. *Genes Dev.* **16**, 2639-2649.
Tournier, S. and Millar, J. B. A. (2000). A role for the START gene-specific transcription factor complex in the inactivation of cyclin B and Cut2 destruction. *Mol. Biol. Cell* **11**, 3411-3424.
Walworth, N. C. and Bernards, R. (1996). Rad-dependent response of the chk1-encoded protein kinase at the DNA damage checkpoint. *Science* **271**, 353-356.
Wan, S. and Walworth, N. C. (2001). A novel genetic screen identifies checkpoint-defective alleles of *Schizosaccharomyces pombe* chk1. *Curr. Genet.* **38**, 299-306.
Wang, L., Guo, Q., Fisher, L. A., Liu, D. and Peng, A. (2015). Regulation of polo-like kinase 1 by DNA damage and PP2A/B55α. *Cell Cycle* **14**, 157-166.
Whitehall, S., Stacey, P., Dawson, K. and Jones, N. (1999). Cell cycle-regulated transcription in fission yeast: Cdc10-Res protein interactions during the cell cycle and domains required for regulated transcription. *Mol. Biol. Cell* **10**, 3705-3715.
Wuarin, J., Buck, V., Nurse, P. and Millar, J. B. A. (2002). Stable association of mitotic cyclin B/Cdc2 to replication origins prevents endoreduplication. *Cell* **111**, 419-431.
Yamaguchi, S., Murakami, H. and Okayama, H. (1997). A WD repeat protein controls the cell cycle and differentiation by negatively regulating Cdc2/B-type cyclin complexes. *Mol. Biol. Cell* **8**, 2475-2486.
Yamaguchi, S., Okayama, H. and Nurse, P. (2000). Fission yeast Fizzy-related protein srw1p is a G1-specific promoter of mitotic cyclin B degradation. *EMBO J.* **19**, 3945-3955.
Yamano, H., Kitamura, K., Kominami, K., Lehmann, A., Katayama, S., Hunt, T. and Toda, T. (2000). The spike of S phase cyclin Cig2 expression at the G1-S border in fission yeast requires both APC and SCF ubiquitin ligases. *Mol. Cell* **6**, 1377-1387.
Yanagida, M. (2009). Cellular quiescence: are controlling genes conserved? *Trends Cell Biol.* **19**, 705-715.
Zhu, Y., Takeda, T., Whitehall, S., Peat, N. and Jones, N. (1997). Functional characterization of the fission yeast Start-specific transcription factor Res2. *EMBO J.* **16**, 1023-1034.